CrossMark

ORIGINAL ARTICLE

Transient delay of radiation-induced apoptosis by phorbol acetate

Gunilla Olsson[1] · Stefan Czene[1] · Siamak Haghdoost[1] · Mats Harms-Ringdahl[1]

Abstract The mechanisms of interference of a model tumour promoter 12-O-tetra-decanoylphorbol-13-acetate (TPA) with radiation-induced apoptosis in human peripheral lymphocytes have been investigated. The cells were treated with TPA under various conditions and thereafter exposed to a single lethal dose of gamma radiation. Morphological and biochemical changes characteristic of apoptosis were followed up to 72 h of post-irradiation time. Acute exposure to low concentration of TPA resulted in delay in the onset of radiation-induced apoptosis (determined as morphological changes and rate of mitochondrial demise) by 24–48 h as compared to the irradiated, sham TPA-treated cells. The time course of this delay correlated well with confinement of the p53 protein to the cytoplasm and increase in bcl-2 levels at the nuclear periphery of irradiated cells. Our results indicate that confinement of p53 in the cytoplasm is one of the potential mechanisms by which TPA interferes with the process of radiation-induced apoptosis in human lymphocytes.

Keywords Human lymphocytes · Radiation · 12-O-tetra-decanoylphorbol-13-acetate · Apoptosis · p53 · bcl-2 · Mitochondria

✉ Stefan Czene
  Stefan.Czene@su.se

[1] Department of Molecular Biosciences, Centre for Radiation Protection Research, The Wenner-Gren Institute, Stockholm University, 106 91 Stockholm, Sweden

Introduction

Ionizing radiation is a potent inducer of apoptosis in human peripheral lymphocytes (HPL) in vivo (Delic et al. 1995) and in vitro (Meijer et al. 1999) through both p53-dependent and p53-independent mechanisms (Seki et al. 1994). Disturbances in the regulation of apoptosis are involved in the pathogenesis of a variety of human diseases (Thompson 1995) including cancer (Evan and Vousden 2001). Several studies implicated inhibition of apoptosis as a mechanism of tumour promotion (Wright et al. 1993; Nguyen-Ba and Vasseur 1999). Indeed, previous studies had shown that stimulation of irradiated HPL by growth factors (Meijer et al. 1999) or mitogens (Carloni et al. 2001) leads to a less efficient induction of apoptosis and increased survival at the expense of genomic fidelity. Of note, mitogen-activated protein kinases (MAPK), which include the extracellular signal-regulated kinases (ERK), p38 and c-Jun amino terminal kinases (JNK), are significant mediators of signals triggered by cytokines, growth factors and environmental stress (Rincon et al. 2000). Modulation of the MAPK signalling pathway has been shown to have profound effects on both radiation-(Carter et al. 1998) and receptor-mediated apoptosis (Holmstrom et al. 1998).

Many of the radiation-induced early-response genes are regulated by the protein kinase C (PKC)-mediated signalling pathway (Schmidt-Ullrich et al. 2000). The cross-talk among PKC-activated proteins and various stress response pathways is exemplified by several reports on the interference of TPA with apoptosis (Hong et al. 1999). TPA is a powerful tumour promoter (Reiners and Singh 1997) that effectively activates protein kinase C by mimicking its natural substrate diacylglycerol (DAG). Albeit TPA may promote apoptosis under certain conditions (Garzotto et al. 1998) more often an inhibitory action of

🖄 Springer

this compound was observed (Sordet et al. 1999; Shen et al. 1998). Our results presented herein show that depending on concentration and time the effect of TPA on radiation-induced apoptosis in HPL may vary to a great extent, ranging from clear-cut cytotoxic effects to significant impairment of radiation-induced apoptosis.

Materials and methods

Isolation and cultivation of lymphocytes

HPL were isolated from freshly collected buffy coats by gradient centrifugation in Ficoll-Paque (Pharmacia). Adherent monocytes were removed by short (1–3 h) incubation in culture flasks (NunClon) at a cell density of 3×10^6 cells/ml in R1 medium (RPMI 1640 medium supplemented with Glutamax-I, 100 IU/ml of penicillin, 100 µg/ml of streptomycine sulphate and 1 % of heat-inactivated foetal bovine serum, all from Gibco RL, Life Technologies). The cells were kept in a CO_2 incubator at 37 °C, 5 % CO_2 and 80 % humidity (standard incubation conditions). After the pre-incubation, the cells were washed, counted and resuspended in R10 medium (the same as the R1 medium except containing 10 % FBS) at a cell density 3×10^6 cells/ml medium. Cell counts and viability were determined by trypan blue staining.

TPA treatment protocols and irradiation

Lymphocytes were exposed acutely (15 min) or chronically (24 h) to low (4 nM) and high (100 nM) concentration of TPA in cell culture medium at 37 °C (TPA+ cells). Control (TPA−) cells were treated in a similar manner as TPA+ cells, except that only the corresponding volume of DMSO was added to the culture medium. The concentration of DMSO was kept in all experiments below 0.01 % in order to avoid undesirable effects on the viability of cells. The cells were centrifuged, washed and resuspended in TPA/DMSO-free medium. Directly afterward, both TPA+ and the TPA− cells were given a dose of 3 Gy at room temperature using a ^{137}Cs γ-radiation source. Control cultures of TPA+ and TPA− cells were sham-exposed.

Determination of apoptosis

Morphological and biochemical changes, characteristic of apoptosis, were studied in the lymphocyte cultures up to 72 h of post-irradiation time. Chromatin condensation, cell fragmentation and changes in membrane permeability were visualized by staining the cells with a mixture of fluorescent dyes H-33342 and propidium iodide (Molecular Probes), at final concentrations 2.5 and 1 µg/ml,

respectively. The slides were coded, and at least 200 cells per sample were scored for the presence of normal, early and late apoptotic and necrotic cells according to the criteria previously described (Czene et al. 2002).

Measurements of mitochondrial membrane potential

Disruption of the mitochondrial membrane potential was detected by staining control and irradiated lymphocytes by the reduced form of chloromethyl-X-rosamine ($CMXH_2$-ROS) (Molecular Probes). Briefly, 5×10^5 cells were centrifuged and resuspended in 1 ml of warm (37 °C) R/10 medium containing $CMXH_2ROS$ (150 nM). As a negative control, similar aliquot of cells was resuspended in 1 ml of R/10 medium containing $CMXH_2ROS$ and the mitochondrial uncoupling agent carbonyl cyanide m-chlorophenyl-hydrazone (mCICCP) at concentrations 150 nM and 50 µM, respectively. The cells were kept for 15 min at standard incubation conditions in dark, washed in warm phosphate-buffered saline (PBS) and fixed with 1 % freshly made paraformaldehyde in PBS for 15 min at room temperature. About 20×10^3 cells were mounted in Slow-Fade (Molecular Probes) medium on object slides, and computer images were acquired for analysis. The image analysis system consisted of a Hamamatsu C4742-95 CCD camera coupled to a Nikon E800 fluorescence microscope and dedicated image analysis program (Openlab). The disruption of mitochondrial membrane potential was assessed as decrease in incorporation of $CMXH_2ROS$ to the mitochondrial membrane. Cells incubated with mCICCP and $CMXH_2ROS$ were used to make a threshold as negative control.

Preparation of total protein extracts and subfractionation to cytosolic and nuclear extracts

At the time points of morphological assessment total cellular lysates were prepared. Briefly, $1–5 \times 10^6$ cells per sample were collected by low-speed centrifugation, washed in ice-cold PBS and lysed in PBS-T (PBS supplied with 0.5 % Triton-X 100). In experiments aimed at detection of subcellular localization of the protein of interest, nuclear and cytoplasmic lysates were prepared essentially as described previously (Dyer and Herzog 1995). Briefly, lymphocytes ($5–10 \times 10^7$) were collected by low-speed centrifugation at 4 °C, washed with PBS and lysed in 100 µl of 0.32 M sucrose, 3 mM CaCl 2, 2 mM magnesium acetate, 0.1 mM EDTA, 10 mM Tris-HCl, pH 8.0, 1 mM DTT, 0.5 % (v/v) Nonidet P-40 (sucrose buffer I). Nuclei were pelleted from the lysates by centrifugation at 500g for 5 min at 4 °C. Cytoplasmic proteins were

extracted by addition of 0.2 volume of 5× cytoplasmic extraction buffer (0.15 M HEPES, pH 7.9, 0.7 M KCl, 0.015 mM $MgCl_2$) to the supernatant and centrifugation at 12,000×g for 15 min at 4 °C. To the resulting supernatant, glycerol was added to a final concentration of 25 % (v/v) and the cytosolic extracts stored at −80 °C. The nuclei were once washed with sucrose buffer I lacking Nonidet P-40 and resuspended in 40 μl/5 × 10^7 cells of low-salt buffer (20 mM HEPES, pH 7.9, 1.5 mM $MgCl_2$, 20 mM KCl, 0.5 mM DTT and 25 % glycerol). Nuclear proteins were extracted by addition of 40 μl of high-salt buffer (20 mM HEPES–NaOH, pH 7.9, 1.5 mM $MgCl_2$, 0.8 M KCl, 0.2 mM EDTA, 1 % Nonidet P-40 and 0.5 mM DTT) and incubation of the resulting mixture at 4 °C for 20 min. Afterward, the mixture was diluted 1:2.5 with diluent buffer (25 mM HEPES–NaOH, pH 7.6, 0.2 mM EDTA, 0.5 mM DTT and 25 % glycerol) and centrifuged at 12,000×g for 15 min at 4 °C, and the nuclear extracts (supernatant) were stored at −80 °C. In order to avoid undesirable protein degradation, all buffers were supplemented with a cocktail of EDTA-free protease inhibitors (Roche Diagnostics) according to the manufacturer's recommendation. Protein concentrations in the cell lysates were determined using the DC Protein Assay Kit (Bio-Rad), as recommended by the manufacturer.

Western blot analysis

A total of 25-μg aliquots of protein samples per lane were resolved on sodium dodecyl sulphate (SDS) polyacrylamide gels and the separated proteins transferred to nitrocellulose membrane for immunochemical analysis. The membranes were incubated 1 h at room temperature in 10 mM TRIS, 150 mM NaCl, pH 7.4 (TBS) containing 5 % non-fat milk powder and thereafter probed for the presence of p53 and bcl-2 proteins. Signal from the constitutively expressed actin was used as a loading control. The following mouse anti-human monoclonal antibodies were used (at final concentrations indicated in parentheses): anti-bcl-2 (1 μg/ml), anti-p53 (0.1 μg/ml) and anti-actin (1.5 μg/ml), all from Santa Cruz Biotechnologies. After 1 h of incubation, the membranes were washed in four consecutive changes of TBS+ 0.1 % Tween-20. The antigen–primary antibody complexes were thereafter visualized by means of a horseradish peroxidase-conjugated anti-mouse antibody and ECL detection system (Amersham) according to the manufacturer's instructions. The dilutions of secondary antibody were 1:3000 for detection of bcl-2; for the detection of p53 and actin, we used a 1:5000 dilution. All antibody incubations were carried out in TBS+ 0.1 % Tween-20 at room temperature.

Chemiluminescent signals were quantified using the Quantiscan for Windows software package (Biosoft,

Oxford, UK). The protein analyses were repeated in least three independent experiments; the obtained values were normalized to the corresponding actin signal.

Immunofluorescence staining of cells

About one million lymphocytes were centrifuged for 10 min at 120 g and the pellet resuspended in PBS. The cells were fixed by freshly prepared 3 % formaldehyde during 15 min at room temperature and then centrifuged for 10 min 120g. The fixed cells were allowed to attach to Superfrost Plus slides (Menzel) and permeabilized during 1 min in methanol–acetone (3:1) at −20 °C. Afterward, the slides were soaked in PBS for 3 min and the non-specific sites blocked with 5 % BSA for 60 min. p53 was detected by incubation with a mouse monoclonal antibody against p53 (DO-1, Santa Cruz) and visualized by Alexa Fluor® 488 goat anti-mouse IgG (H + L) antibody (Molecular Probes). All antibody incubations and washing steps were carried out at room temperature in a humidity chamber. After the final washing step, the cells mounted in Slow-Fade (Molecular Probes). Z-stacks of images were acquired by means of a Nikon (Eclipse E800 and Hamamatsu C-4742-95 CCD camera) microscope with a confocal stage and combined into confocal images by help of a dedicated software package (Openlab).

Results

Interference of TPA with spontaneous and radiation-induced apoptosis

Cultured lymphocytes spontaneously undergo apoptosis at a rate that increases by time of incubation (Czene et al. 2002) most likely due to loss of extracellular survival signalling and reductions in glycolytic metabolism (Plas et al. 2002). Hence, our initial experiments were aimed to determine how various TPA treatment protocols affect the rate of spontaneously occurring apoptosis in lymphocyte cultures. Acute (15 min) and chronic (24 h) exposures to high (100 nM) concentration of TPA as well as chronic exposure to low (4 nM) TPA concentration resulted—to a varying extent—in increase in apoptosis rate above that of spontaneously occurring in cultured lymphocytes (Fig. 1). The cytotoxic effect of TPA treatment was further enhanced by radiation (data not shown). Previous studies demonstrated the depletion of PKC by protracted exposures (12–24 h) to TPA (Hrzenjak and Shain 1995; Isonishi et al. 2000), most likely through the activation of the ubiquitin pathway. Hence, it can be assumed that the cytotoxic effect of TPA in our experimental model is attributable to PKC depletion.
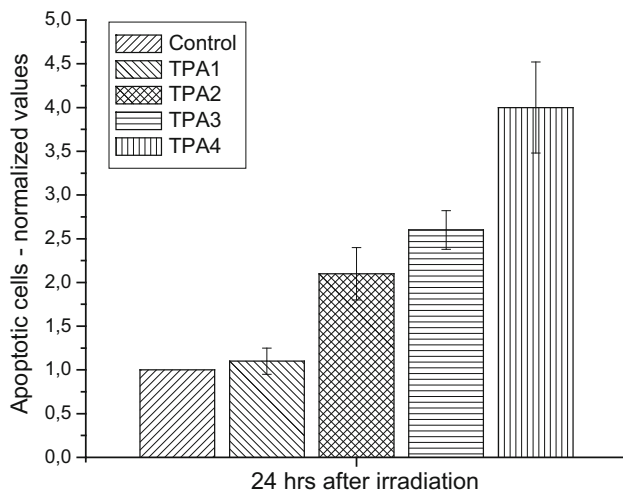
Fig. 1 Effect of various TPA treatment protocols on the rate of spontaneously occurring apoptosis in human lymphocytes. After the exposure of cells to the indicated TPA concentration and time, the cells were centrifuged and resuspended in TPA-free medium. The number of apoptotic cells was determined after 24-h incubation in TPA-free medium and the values normalized to the apoptosis rate in the control untreated cells. The *error bars* indicate SEs of measurement among four independent experiments. C—control cells; TPA1—4 nM TPA, 15 min; TPA2—100 nM TPA, 15 min; TPA3—4 nM TPA, 24 h; TPA4—100 nM TPA, 24 h

Acute exposure to low TPA concentration had no significant effect on the rate of background apoptosis in control cells (Fig. 1; Table 1). However, at these exposure conditions, there was a significant reduction of apoptosis in irradiated TPA+ cultures as compared to those irradiated in the absence of TPA (Table 1). The protective effect of TPA was most pronounced between the 9th and 48th hours of post-irradiation incubation.

Changes of mitochondrial membrane potential

Diverse apoptotic stimuli, e.g. cytotoxic drugs, DNA-damaging agents, heat shock, hypoxia, growth factor withdrawal, irradiation and death domain receptor signalling, converge on mitochondria and induce release of pro-apoptotic factors into the cytoplasm (Robertson and Orrenius 2000). Our measurements of mitochondrial membrane potential (Table 1) revealed a delayed demise of the mitochondrial function in irradiated TPA+ cells compared to irradiated TPA− cells. The time kinetics of mitochondrial changes was very similar to that observed for the onset of the morphological changes. The general tendency of higher numbers of cells with impaired mitochondria compared to those of cells displaying morphological changes characteristic of apoptosis indicates the important role of mitochondrial changes in early stages of radiation-induced apoptosis in HPL. Moreover, the data also implicate that TPA acts upstream of the events that lead to the loss of mitochondrial membrane potential.

Radiation-induced changes in amount and localization of p53 and bcl-2 proteins

Radiation-induced apoptosis in HPL can be mediated by p53-dependent or p53-independent mechanisms (Seki et al. 1994). Principal downstream elements of the DNA-damage-induced, p53-driven apoptotic pathway are modulatory interactions between the members of the bcl-2 gene family, release of mitochondrial pro-apoptotic factors and activation of caspases. As p53 is a regulator of bcl-2 and bax gene expression in vitro and in vivo (Miyashita et al. 1994b), we have examined radiation-induced changes in the levels of p53 and bcl-2 proteins in total cell lysates. While the levels of p53 in the non-irradiated cells were around the limit of

Table 1 Morphological changes and loss of mitochondrial membrane potential in control and irradiated lymphocytes

Time (h)	Control				Irradiated			
	TPA−		TPA+		TPA−		TPA+	
	Apoptotic	CMXH$_2$ROS (−)	Apoptotic	CMXH$_2$ROS (−)	Apoptotic	CMXH$_2$ROS (−)	Apoptotic	CMXH$_2$ROS (−)
0	3.8 ± 0.5	4.1 ± 0.7	3.9 ± 0.5	4.8 ± 0.7	5 ± 0.4	3.1 ± 0.7	6 ± 0.5	5.4 ± 2.2
6	4.2 ± 0.3	5.5 ± 1.2	3.7 ± 0.3	3.9 ± 0.6	3.8 ± 1.3	5.5 ± 1.1	4 ± 0.8	6.5 ± 0.7
9	3.5 ± 0.4	5.6 ± 0.9	4 ± 0.5	5.1 ± 0.9	7.5 ± 2.8*	9.2 ± 1.6**	3.4 ± 0.4[†]	6.1 ± 0.6[†]
24	5 ± 1.1	7.1 ± 1.1	5.5 ± 1.3	6.9 ± 1.1	26 ± 3.5***	31.3 ± 3.1***	16.5 ± 2.8[††]	15.8 ± 1.5[†††]
48	12 ± 2	14.9 ± 2.3	10 ± 2.5	13.1 ± 2.1	45 ± 5.4***	51 ± 0.9***	33 ± 1.8[††]	45.3 ± 2.7[†]
72	14 ± 2.3	17.1 ± 3.1	15 ± 2.6	16.5 ± 1.3	72 ± 2.4***	82.1 ± 2.8***	68.5 ± 3.4	75.1 ± 3.5

The values represent means ± SEs from four donors. The significance of differences between the employed treatments were investigated by Student's paired *t* test

* $P < 0.05$; ** $P < 0.01$; *** $P < 0.001$ (in comparison with—TPA control cultures); [†] $P < 0.05$; [††] $P < 0.01$; [†††] $P < 0.001$ (in comparison with—TPA irradiated cultures)

detection, radiation induced a rapid increase in the p53 levels within 3 h after irradiation (Fig. 2). The expression of p53 in irradiated TPA− cells reached its maximum 6–24 h after irradiation and declined to the control levels 48–72 h after irradiation. The time course of p53 induction in the irradiated TPA+ cells was more protracted, with elevated p53 levels up to 48 h (Fig. 2) and decrease to the control level 72–96 h after irradiation (data not shown).

As p53 induction was observed already a few hours after irradiation, we were interested which opposing signals could abrogate the p53-driven apoptotic pathway in the irradiated TPA+ cells. Regulation of p53 activity can be achieved by increase in protein concentration, conformational changes and cytoplasmic/nuclear shuttling (Liang and Clarke 2001). Nuclear accumulation of p53 protein is pivotal for the mediation of its cellular effects (Sugano et al. 1995; Shaulsky et al. 1990; Fritsche et al. 1993), and abnormal cytoplasmic sequestration of p53 has been suggested as a mutation-independent mechanism of p53 inactivation (Moll et al. 1996). Fractionation of protein content into nuclear and cytoplasmic lysates (Fig. 3) as well as confocal images (Fig. 4) revealed differences in the nuclear localization of p53 among irradiated TPA+ and TPA− cells. While the majority of p53 protein showed nuclear localization in irradiated TPA− cells during the post-irradiation incubation, in irradiated TPA+ cells p53 was localized mostly in the cytoplasm up to 48 h after irradiation, whereupon it shifted to mainly nuclear accumulation (Figs. 3, 4). It should be stressed, however, that not all TPA+ cells showed cytosolic confinement of p53 indicating that this phenomenon could be characteristic for a certain subpopulation of HPL.
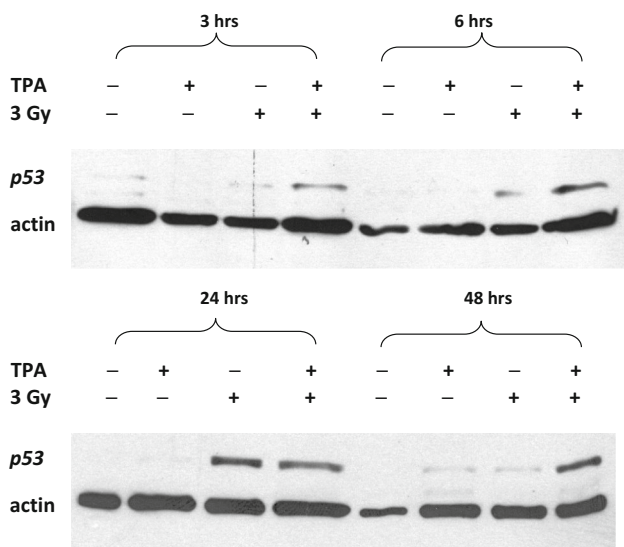
The bcl-2 family of cytoplasmic proteins—through interactions between its anti- and pro-apoptotic members—is thought to be one of the major anti-apoptotic regulators in the cell. Systemic overexpression of bcl-2 in the haematopoietic system has been shown to increase the resistance of mice to lethal challenges such as irradiation (Ogilvy et al. 1999). An earlier study has suggested a gatekeeper function of the bcl-2 protein at the nuclear membrane by inhibiting nuclear import of induced wild-type p53 protein following genotoxic damage (Beham et al. 1997). While there were no significant changes in the expression of bcl-2 protein in the total cell lysates (data not shown), upon fractionation of the cellular protein content into nuclear and cytoplasmic lysates, significant increase in bcl-2 in the nuclear fraction of irradiated cells was detected (Fig. 3). This increase became marked in both TPA− and TPA+ cells already 1 h after irradiation, reached its maximum about 24 h after irradiation and slowly declined to the control levels at the 48–72 h of post-irradiation time. This increase was quite unexpected, as the presence of the p53-dependent negative response element in the bcl-2 gene (Miyashita et al. 1994a) would implicate that up-regulation of p53 would lead down-regulation of bcl-2 expression. Yet, irradiation resulted in increase in bcl-2 levels in the nuclear fraction in both TPA− and TPA+ cells (Fig. 3). While in the case of TPA− cells this increase seems to depend on de novo synthesis as the cytosolic levels of bcl-2 have also increased, in TPA+ cells the increase is accompanied with a drop of cytosolic bcl-2 levels 1 h after the irradiation (Fig. 3, lower panel). Of note, staining of the irradiated cells with the potential-independent mitochondrial stain Mitotracker Green showed the preferential localization of mitochondria close to the nuclear membrane (data not shown). As the bcl-2 protein frequently associates with the mitochondrial membrane, this could lend a partial explanation for the observed pattern of localization. Elevated bcl-2 levels at the nuclear periphery could also originate from TPA-induced up-regulation of PKC as it has recently been shown that the bcl-2 mRNA is endowed by an adenine- and uracil-rich element (ARE), a common element responsible for mRNA decay modulation (Schiavone et al. 2000). The same study demonstrated that the activity of bcl-2 ARE is influenced by PKC, since the addition of both DAG and TPA markedly attenuated its destabilizing potential.

Discussion

We show here that short pre-treatment by low concentration of TPA transiently decreases the rate of radiation-induced apoptosis in human peripheral lymphocytes. This decrease correlated well with the restricted nuclear entry of
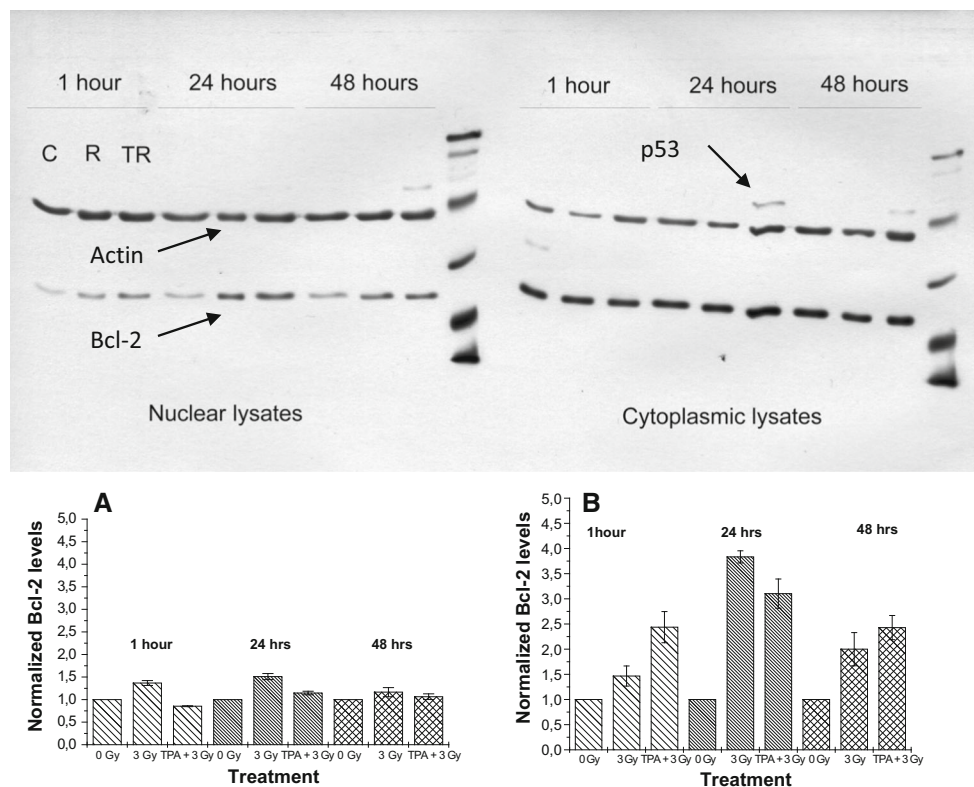

Fig. 2 Western blot analysis of p53 expression in total cell lysates. The TPA treatment indicates acute exposure to low TPA concentration (4 nM, 15 min)

Fig. 3 The *upper panel* depicts p53 and bcl-2 protein levels in nuclear and cytoplasmic fractions of lymphocytes, detected by Western blot analysis. TPA-treated and sham-treated lymphocytes were exposed to 3 Gy of radiation and samples collected for protein analysis at 1, 24 and 48 h of post-irradiation incubation. C—control cells; R—cells irradiated with 3 Gy; TR—cells pre-exposed to low concentration of TPA (4 nM, 15 min) and irradiated afterward with 3 Gy. Densitometric evaluation of time-dependent changes of bcl-2 protein levels in nuclear (**a**) and cytoplasmic (**b**) fractions of lymphocytes is shown in the *lower panel*. The values are normalized to the respective actin signals in the same lane

the p53 protein and increase in bcl-2 levels at the nuclear periphery of irradiated cells. This is in line with a previous study that reported on bcl-2-mediated inhibition of p53 nuclear import following DNA damage in the human prostate carcinoma cell line LNCaP (Beham et al. 1997). Still, the observed changes in subcellular levels of bcl-2 in HPL seem to be necessary but not sufficient for blocking of the nuclear accumulation of p53, as the latter has been observed only in TPA-treated cells. Of note, TPA is known to induce c-myc expression via PKC activation and it has previously been demonstrated that bcl-2 and c-myc can cooperate in blocking the p53 entry into the nucleus and prevent p53-induced apoptosis and growth arrest of breast cancer cells (Ryan et al. 1994). One should bear in mind, however, several contradictory reports from other cell models. Mitogen-activated lymphocytes and cycling T lymphoma cells from p53-deficient mice exhibited significant apoptotic cell death following exposure to ionizing radiation or DNA-damaging drugs (Hendry and West 1997). These findings suggest that p53 is not the only mediator of apoptotic cell death upon DNA damage.

Moreover, it has previously been shown that overexpression of bcl-2 protein increases the half-life of Bax protein in some (but not all) cell types (Miyashita et al. 1995) that would circumvent the anti-apoptotic effect of elevated bcl-2 levels.

Our results indicate that TPA may interfere with the process of radiation-induced cell death, at least partly, through activation of signal transduction mechanisms that are able to inhibit apoptotic signalling at a stage upstream of mitochondrial demise. This is in line with a previous study on radiation-induced apoptosis of Jurkat cells (Shonai et al. 2002) that demonstrated the protective effect of the MEK/ERK pathway on ionizing radiation-induced loss of mitochondrial membrane potential. It should be stressed, however, that HPL which can be rescued from radiation-induced cell death by stimulation with mitogens (Meijer et al. 1999) may already contain a significant number of DNA fragments (Czene et al. 2002). Inhibition of apoptosis in its early phases therefore could increase the risk of formation of chromosomal aberrations in cells under stimulatory pressure of the

Fig. 4 Confocal microscopy images of p53 distribution in control (**a**) and irradiated TPA+ (**b**) lymphocytes. *Upper row—24 h; Middle row—48 h; Lower row—72 h*
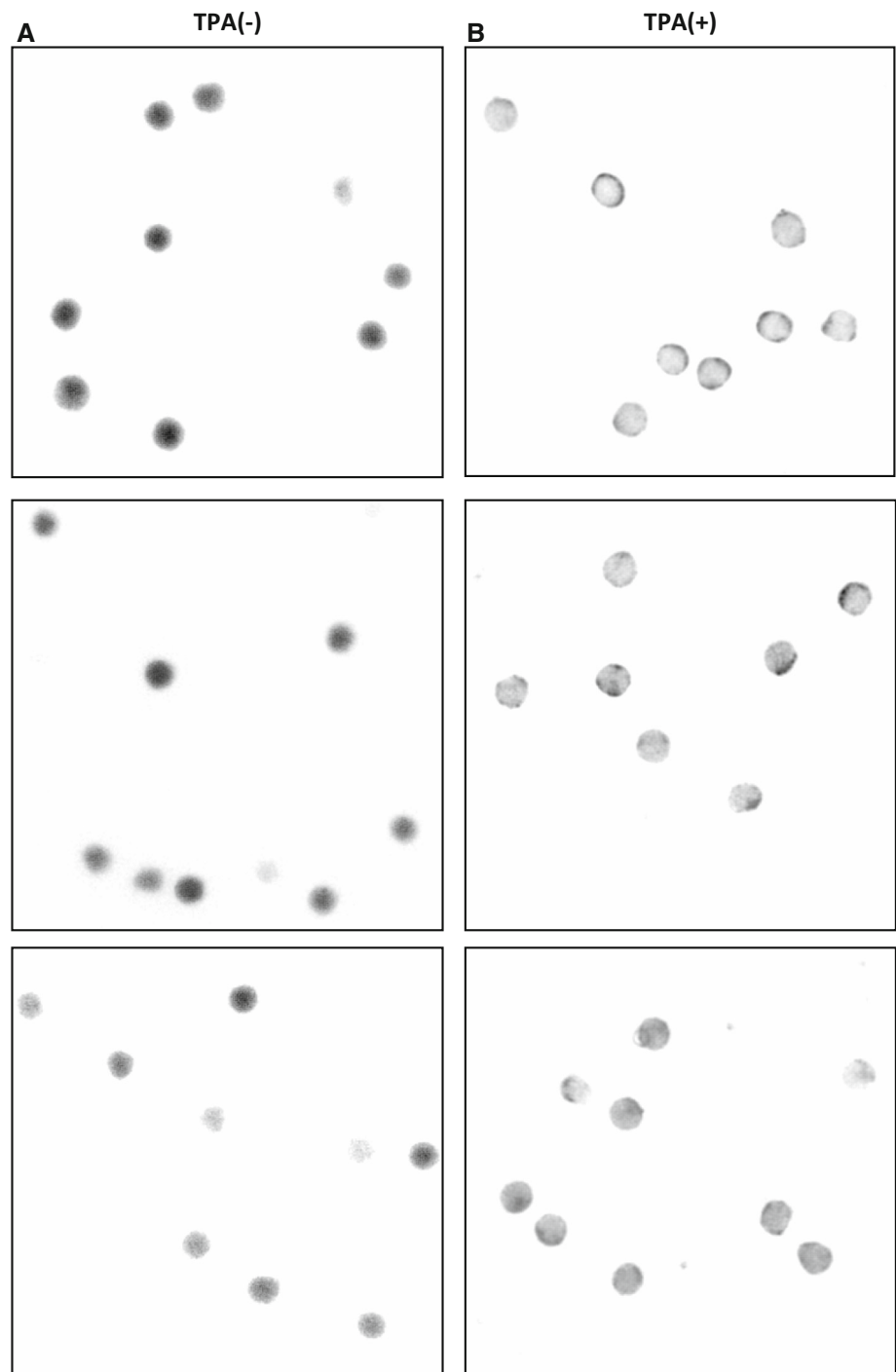
immune system and result in a carry-over of genetic damage to daughter cells.

References

Beham A, Marin MC, Fernandez A, Herrmann J, Brisbay S, Tari AM, Lopez-Berestein G, Lozano G, Sarkiss M, McDonnell TJ (1997) Bcl-2 inhibits p53 nuclear import following DNA damage. Oncogene 15(23):2767–2772

Carloni M, Meschini R, Ovidi L, Palitti F (2001) PHA-induced cell proliferation rescues human peripheral blood lymphocytes from X-ray-induced apoptosis. Mutagenesis 16(2):115–120

Carter S, Auer KL, Reardon DB, Birrer M, Fisher PB, Valerie K, Schmidt-Ullrich R, Mikkelsen R, Dent P (1998) Inhibition of the mitogen activated protein (MAP) kinase cascade potentiates cell killing by low dose ionizing radiation in A431 human squamous carcinoma cells. Oncogene 16(21):2787–2796

Czene S, Testa E, Nygren J, Belyaev I, Harms-Ringdahl M (2002) DNA fragmentation and morphological changes in apoptotic human lymphocytes. Biochem Biophys Res Commun 294(4):872–878

Delic J, Magdelenat H, Barbaroux C, Chaillet MP, Dubray B, Gluckman E, Fourquet A, Girinsky T, Cosset JM (1995) In vivo induction of apoptosis in human lymphocytes by therapeutic fractionated total body irradiation. Br J Radiol 68(813):997–1003

Dyer RB, Herzog NK (1995) Isolation of intact nuclei for nuclear extract preparation from a fragile B-lymphocyte cell line. Biotechniques 19(2):192–195

Evan GI, Vousden KH (2001) Proliferation, cell cycle and apoptosis in cancer. Nature 411(6835):342–348

Fritsche M, Haessler C, Brandner G (1993) Induction of nuclear accumulation of the tumor-suppressor protein p53 by DNA-damaging agents. Oncogene 8(2):307–318

Garzotto M, White-Jones M, Jiang Y, Ehleiter D, Liao WC, Haimovitz-Friedman A, Fuks Z, Kolesnick R (1998) 12-O-tetradecanoylphorbol-13-acetate-induced apoptosis in LNCaP cells is mediated through ceramide synthase. Cancer Res 58(10):2260–2264

Hendry JH, West CM (1997) Apoptosis and mitotic cell death: their relative contributions to normal-tissue and tumour radiation response. Int J Radiat Biol 71(6):709–719

Holmstrom TH, Chow SC, Elo I, Coffey ET, Orrenius S, Sistonen L, Eriksson JE (1998) Suppression of Fas/APO-1-mediated apoptosis by mitogen-activated kinase signaling. J Immunol 160(6):2626–2636

Hong M, Lai MD, Lin YS, Lai MZ (1999) Antagonism of p53-dependent apoptosis by mitogen signals. Cancer Res 59(12):2847–2852

Hrzenjak M, Shain SA (1995) Protein kinase C-dependent and -independent pathways of signal transduction in prostate cancer cells: fibroblast growth factor utilization of a protein kinase C-independent pathway. Cell Growth Differ 6(9):1129–1142

Isonishi S, Ohkawa K, Tanaka T, Howell SB (2000) Depletion of protein kinase C (PKC) by 12-O-tetradecanoylphorbol-13-acetate (TPA) enhances platinum drug sensitivity in human ovarian carcinoma cells. Br J Cancer 82(1):34–38

Liang SH, Clarke MF (2001) Regulation of p53 localization. Eur J Biochem 268(10):2779–2783

Meijer AE, Saeidi AB, Zelenskaya A, Czene S, Granath F, Harms-Ringdahl M (1999) Influence of dose-rate, post-irradiation incubation time and growth factors on interphase cell death by apoptosis and clonogenic survival of human peripheral lymphocytes. Int J Radiat Biol 75(10):1265–1273

Miyashita T, Harigai M, Hanada M, Reed JC (1994a) Identification of a p53-dependent negative response element in the bcl-2 gene. Cancer Res 54(12):3131–3135

Miyashita T, Krajewski S, Krajewska M, Wang HG, Lin HK, Liebermann DA, Hoffman B, Reed JC (1994b) Tumor suppressor p53 is a regulator of bcl-2 and bax gene expression in vitro and in vivo. Oncogene 9(6):1799–1805

Miyashita T, Kitada S, Krajewski S, Horne WA, Delia D, Reed JC (1995) Overexpression of the Bcl-2 protein increases the half-life of p21Bax. J Biol Chem 270(44):26049–26052

Moll UM, Ostermeyer AG, Haladay R, Winkfield B, Frazier M, Zambetti G (1996) Cytoplasmic sequestration of wild-type p53

protein impairs the G1 checkpoint after DNA damage. Mol Cell Biol 16(3):1126–1137

Nguyen-Ba G, Vasseur P (1999) Epigenetic events during the process of cell transformation induced by carcinogens (review). Oncol Rep 6(4):925–932

Ogilvy S, Metcalf D, Print CG, Bath ML, Harris AW, Adams JM (1999) Constitutive Bcl-2 expression throughout the hematopoietic compartment affects multiple lineages and enhances progenitor cell survival. Proc Natl Acad Sci USA 96(26):14943–14948

Plas DR, Rathmell JC, Thompson CB (2002) Homeostatic control of lymphocyte survival: potential origins and implications. Nat Immunol 3(6):515–521

Reiners JJ Jr, Singh KP (1997) Susceptibility of 129/SvEv mice in two-stage carcinogenesis protocols to 12-O-tetradecanoylphorbol-13-acetate promotion. Carcinogenesis 18(3):593–597

Rincon M, Flavell RA, Davis RA (2000) The JNK and P38 MAP kinase signaling pathways in T cell-mediated immune responses. Free Radic Biol Med 28(9):1328–1337

Robertson JD, Orrenius S (2000) Molecular mechanisms of apoptosis induced by cytotoxic chemicals. Crit Rev Toxicol 30(5):609–627

Ryan JJ, Prochownik E, Gottlieb CA, Apel IJ, Merino R, Nunez G, Clarke MF (1994) c-myc and bcl-2 modulate p53 function by altering p53 subcellular trafficking during the cell cycle. Proc Natl Acad Sci USA 91(13):5878–5882

Schiavone N, Rosini P, Quattrone A, Donnini M, Lapucci A, Citti L, Bevilacqua A, Nicolin A, Capaccioli S (2000) A conserved AU-rich element in the 3′ untranslated region of bcl-2 mRNA is endowed with a destabilizing function that is involved in bcl-2 down-regulation during apoptosis. FASEB J 14(1):174–184

Schmidt-Ullrich RK, Dent P, Grant S, Mikkelsen RB, Valerie K (2000) Signal transduction and cellular radiation responses. Radiat Res 153(3):245–257

Seki H, Kanegane H, Iwai K, Konno A, Ohta K, Yachie A, Taniguchi N, Miyawaki T (1994) Ionizing radiation induces apoptotic cell death in human TcR-gamma/delta+ T and natural killer cells without detectable p53 protein. Eur J Immunol 24(11):2914–2917

Shaulsky G, Goldfinger N, Ben-Ze'ev A, Rotter V (1990) Nuclear accumulation of p53 protein is mediated by several nuclear localization signals and plays a role in tumorigenesis. Mol Cell Biol 10(12):6565–6577

Shen SC, Huang TS, Jee SH, Kuo ML (1998) Taxol-induced p34cdc2 kinase activation and apoptosis inhibited by 12-O-tetradecanoylphorbol-13-acetate in human breast MCF-7 carcinoma cells. Cell Growth Differ 9(1):23–29

Shonai T, Adachi M, Sakata K, Takekawa M, Endo T, Imai K, Hareyama M (2002) MEK/ERK pathway protects ionizing radiation-induced loss of mitochondrial membrane potential and cell death in lymphocytic leukemia cells. Cell Death Differ 9(9):963–971

Sordet O, Bettaieb A, Bruey JM, Eymin B, Droin N, Ivarsson M, Garrido C, Solary E (1999) Selective inhibition of apoptosis by TPA-induced differentiation of U937 leukemic cells. Cell Death Differ 6(4):351–361

Sugano T, Nitta M, Ohmori H, Yamaizumi M (1995) Nuclear accumulation of p53 in normal human fibroblasts is induced by various cellular stresses which evoke the heat shock response, independently of the cell cycle. Jpn J Cancer Res 86(5):415–418

Thompson CB (1995) Apoptosis in the pathogenesis and treatment of disease. Science 267(5203):1456–1462

Wright SC, Zhong J, Zheng H, Larrick JW (1993) Nicotine inhibition of apoptosis suggests a role in tumor promotion. FASEB J 7(11):1045–1051